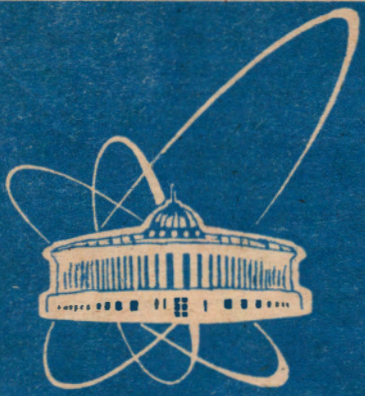

СООБЩЕНИЯ
ОБЪЕДИНЕННОГО
ИНСТИТУТА
ЯДЕРНЫХ
ИССЛЕДОВАНИЙ

Дубна

E2-96-470

M.K.Volkov, E.A.Kuraev, D.Blaschke[1], G.Röpke[1], S.Schmidt[2]

TWO PHOTONS ANNIHILATION OF PIONS AND THE COMPTON EFFECT OFF PIONS IN HOT AND DENSE MEDIUM

[1]MPG Arbeitsgruppe «Theoretische Vielteilchenphysik», Universität Rostock, D-18051, Rostock, Germany

[2]School of Physics and Astronomy Tel Aviv University, 69978 Tel Aviv, Israel

1996

1. Introduction

The investigation of hadron properties at finite temperature and density is very important in order to provide insight into phenomena occuring in the vicinity of the transition to the hypothetical quark-gluon plasma state of matter which is characterized by hadron deconfinement and restoration of chiral symmetry. These studies become particularly interesting since in ultra-relativistic heavy ion collision experiments performed and planned at BNL Brookhaven and CERN Geneva one is able to create matter at the extreme densities and temperatures necessary for the phase transition. Different effects have been discussed as possible signatures for the chiral/deconfinement transition, in particular J/Ψ suppression [1], low-mass dilepton enhancement [2] and strangeness enhancement [3] have been studied. Among the signals of such a transition the photons and dileptons are the most interesting ones since they leave the hot and dense matter at an early stage without suffering strong interactions.

One of the products of heavy ion collisions is the pion gas. Therefore it is interesting to investigate the behaviour of such a gas at large temperature and/or density, in particular the study of its radiation is of interest. The main channel of this radiation is the annihilation of two pions into one photon. With help of this reaction it is possible to study the behaviour of the intermediate ρ- meson under the influence of a hot and dense medium [4, 5, 6]. Among other radiation processes of the pion gas, the annihilation of two pions into two photons is of particular importance. In the vacuum this reaction contributes to the amplitude with noticeable probability for the charged pions only by the Born diagrams. Recently, the importance of this process in a hot medium for the explanation of excess low-mass dileptons has been discussed without assuming ρ- mass shift or quark-substructure effects [7]. However, for large temperature and density the quark-substructure terms (box and σ-pole diagrams) become more important and give a remarkable contribution to the cross section which is comparable to that of the Born terms. It is important to investigate these effects since they could permit a better understanding of the properties of the scalar meson and phemomena connected with deconfinement of hadrons.

The paper is organized as follows: In Section 2 the annihilation process of the two pions into two photons is presented and discussed. It is shown that the σ pole diagram [8–12] plays a very important role at large chemical potential, when $M_\sigma = 2M_\pi$. In Section 3 the Compton effect for the pions is discussed in hot and dense matter.In this section the singularities at the Mott point are investigated.Some proposals for the observation of this property are discussed in sections 4,5. We summarize and conclude in Section 6. In Appendix I there we show that in the amplitude of the process $\pi\pi \to \gamma\gamma$ the singularities are absent at the Mott point. In Appendix II we show that these singularities exist in the Compton effect of the pions and calculate the coefficients of the singular terms.

2. The process $\pi\pi \to \gamma\gamma$ at finite chemical potential

The process $\pi\pi \to \gamma\gamma$ is described by the Born terms (for charged pions, see Fig. 1) and the terms connected with the inner structure of the pions [11, 12] (for charged and neutral pions, see Fig. 2). The $\sigma-$pole diagram (Fig. 2a) and the box diagrams (Fig. 2b-d) are the most important contributions.

The Lagrangian describing the diagrams Fig. 1a,b has the form

$$L = ieA_\mu(\pi^-\partial_\mu\pi^+ - \pi^+\partial_\mu\pi^-) + A_\mu^2\pi^+\pi^-. \tag{1}$$

The vertices of the Fig. 2 in the local approximation in the Nambu–Jiona-Lasinio (NJL) model [13] are described by the following langrangians in local approximation (NJL model) [11, 12, 14, 15].

$$\begin{aligned} L_{box} &= \frac{\alpha}{18\pi F_\pi^2}(\pi^+\pi^- + 5\pi^0\pi^0)F_{\mu\nu}^2, \\ L_{\sigma\pi\pi} &= 2mgZ^{1/2}\cos\gamma\sigma\vec{\pi}^2, \\ L_{\sigma\gamma\gamma} &= \frac{\alpha Z^{-1/2}}{9\pi F_\pi}(5\cos\gamma + \sqrt{2}\sin\gamma)\sigma F_{\mu\nu}^2, \end{aligned} \tag{2}$$

where σ and π are the scalar meson and pion fields, $\alpha = \frac{e^2}{4\pi} = \frac{1}{137}$, $F_{\mu\nu} = \partial_\mu A_\nu - \partial_\nu A_\mu$, the pion decay constant $F_\pi = 93$ MeV, the strong pion coupling constant $g = \frac{m}{F_\pi}$, the dynamical quark mass $m = 280$ MeV. The renormalization coefficient $Z = (1 - \frac{6m^2}{M_{a_1}^2})^{-1}$ is due to the $\pi - a_1$ mixing [11], the mixing angle γ describes the deviation of the singlet-octet mixing angle from the ideal mixing ($\gamma = 23^o$),[15]. At large temperatures T and chemical potentials μ we can set $\gamma = 0$ and $Z = 1$, (see [15, 16]). Then for charged pions the amplitude describing the sum of the Born diagram as well as the σ-pole and the box graphs become

$$\begin{aligned} T_{(\pi(q_1)+\pi(q_2)\to\gamma_\mu(k_1)+\gamma_\nu(k_2))} &= e^2\big[2(g^{\mu\nu} - \frac{q_1^\mu q_2^\nu}{q_1k_1} - \frac{q_2^\mu q_1^\nu}{q_2k_1}) \\ &+ A(g_{\mu\nu}k_1k_2 - k_1^\nu k_2^\mu)\big]e_\mu(k_1)e_\nu(k_2), \end{aligned} \tag{3}$$

where q_i and k_i are the momenta of pions and photons respectively, $e_\mu(k_1)$ and $e_\nu(k_2)$ are the polarizations of the photons.

$$A = \frac{1}{(6\pi F_\pi)^2}\left[\frac{40m^2}{M_\sigma^2 - s - iM_\sigma\Gamma_\sigma}f_1(\mu,T) - f_2(\mu,T)\right] \tag{4}$$

is the contribution of the σ- pole and the box diagram [11, 12, 14]. Mass and width of the σ meson are given as

$$\begin{aligned} M_\sigma^2 &= M_\pi^2 + 4m^2 \\ \Gamma_\sigma &= \frac{3m^4}{2\pi M_\sigma F_\pi^2}Z\sqrt{1 - \frac{4M_\pi^2}{s}}\cos^2\gamma. \end{aligned} \tag{5}$$

The functions f_1 and f_2 describe the dependence of the quark triangle and the quark box diagrams on temperature and chemical potential [14] and are given as follows

$$f_1(\mu,T) = 1 - \frac{3}{2}m^2\int_0^\infty dk\frac{k^3}{E^6}\ln\frac{E+k}{E-k}\Big[n(k,T,\mu) + \bar{n}(k,T,\mu)\Big] \tag{6}$$

$$f_2 = 3m^2\int_0^\infty dk\frac{k^2}{E^5}\Big[1 - n(k,T,\mu) - \bar{n}(k,T,\mu)\Big]. \tag{7}$$

The Fermi distribution function $n(k,\mu,T) = \Big[1+\exp[(E(k)-\mu)/T]\Big]^{-1}$ describes the dependence on temperature and chemical potential for particles and antiparticles of the energy $E(k) = \sqrt{k^2+m^2}$ [16]. The functions $f_i(\mu,T)$ describe the dependence of the triangle $\sigma\gamma\gamma$ and the box quark diagrams on temperature and chemical potential [14]. For the square of the amplitude (3) we obtain

$$\begin{aligned} |T|^2 = 4e^2\big(2 + M_\pi^4\big[&\frac{1}{(k_1q_1)^2} + \frac{1}{(k_2q_1)^2}\big] + 2\frac{(q_1q_2)^2}{(k_1q_1)(k_2q_1)} \\ &-2q_1q_2(\frac{1}{k_1q_1} + \frac{1}{k_1q_2}) + \ \mathrm{Re}\,A\big[3k_1k_2 + \frac{(k_2q_1)^2 - (k_1k_2)(q_1q_2)}{k_1q_1} + \\ &+\frac{(k_1q_1)^2 - (k_1k_2)(q_1q_2)}{k_2q_1}\big] + \frac{|A|^2}{2}(k_1k_2)^2\big). \end{aligned} \tag{8}$$

Let us consider the following coordinate system $|\vec{q}_i| = |\vec{k}| = \omega$, $k_1 = (\omega,\vec{k})$, $k_2 = (\omega,-\vec{k})$,$q_1 = (\omega,\vec{q})$, $q_2 = (\omega,-\vec{q})$, $\omega^2 = M_\pi^2 + \vec{q}^2$, $c = \cos(\vec{q}_1,\vec{k}_1)$, $s = (q_1 + q_2)^2 = 2M_\pi^2 + 2q_1q_2 = 4\omega^2 = 2k_1k_2$, $\omega^2 = s/4$, $\beta^2 = 1 - M_\pi^2/\omega^2 = 1 - 4M_\pi^2/s$, $k_1q_1 = k_2q_2 = \omega^2(1-\beta c)$, $q_1q_2 = s/2 - M_\pi^2, k_2q_1 = k_1q_2 = \omega^2(1+\beta c)$.

The calculation of the cross section for this process gives

$$\begin{aligned} \sigma^{\pi^+\pi^-\to\gamma\gamma} &= \frac{1}{(2\pi)^2}\frac{1}{4s\beta}\int\frac{d^3k_1}{2\omega_1}\frac{d^3k_2}{2\omega_2}\delta^4(q_1+q_2-k_1-k_2)|T|^2 \\ &= \frac{\pi\alpha^2}{s\beta}[4(2 - \beta^2 - \frac{1-\beta^4}{2\beta}\ln\frac{1+\beta}{1-\beta}) \\ &+s(\ \mathrm{Re}\,A)\frac{1-\beta^2}{\beta}\ln\frac{1+\beta}{1-\beta} + \frac{s^2}{4}|A|^2]. \end{aligned} \tag{9}$$

Let us test how the radiation of the photons with the $\omega = 170$Mev ($s = 0.115$Gev^2) will change when we go from vacuum to the case with the finite T and μ. For that we shall calculate the contributions to the total cross section from the Born terms and from structure terms.[1]

Here we shall consider only the main quark-substructure terms and neglect the vector and axial-vector pole diagrams. At first we consider the zero temperature

[1]The value $s = 0.115$Gev^2 ($\omega = 170$ Mev) corresponds to the resonance of the σ-pole term in eq. (4) at the $T = 100$ MeV, $\mu = 270$ MeV ($s = m_\sigma^2$).

and density case with $s = 4M_\pi^2(1+\epsilon)$. In our model [11] we fix the constituent quark mass at $m = 280$ MeV and obtain $M_\sigma = \sqrt{M_\pi^2 + 4m^2} = 580$ MeV. If we consider the low energy reaction when $s = 0.115$ GeV^2, $\epsilon = 0.44$ and $\beta = 0.55$ then we obtain from Eq.(5)

$$M_\sigma \Gamma_\sigma = 0.19 \mathrm{GeV}^2 \tag{10}$$

and the last term of Eq. (9) equals to ($f_1 = f_2 = 1$)

$$\begin{aligned} \frac{\pi\alpha^2}{4s\beta}|s\mathcal{A}|^2 &= \frac{\pi\alpha^2}{4s\beta}\left[(1+\varepsilon)(\frac{M_\pi}{3\pi F_\pi})^2\right]^2\left[\left[\frac{40m^2(M_\sigma^2 - 4M_\pi^2(1+\varepsilon))}{(M_\sigma^2 - 4M_\pi^2(1+\varepsilon))^2 + (M_\sigma\Gamma_\sigma)^2} - 1\right]^2\right. \\ &\left. +(\frac{40m^2 M_\sigma\Gamma_\sigma}{(M_\sigma^2 - 4M_\pi^2(1+\varepsilon))^2 + (M_\sigma\Gamma_\sigma)^2})^2\right] \\ &= \frac{\pi\alpha^2}{4s\beta}0.07. \end{aligned} \tag{11}$$

The interference term is equal to

$$s\mathrm{Re}\mathcal{A} = 0.26. \tag{12}$$

Then for the total cross section we obtain

$$\sigma^{\pi^+\pi^-\to\gamma\gamma} = \frac{\pi\alpha^2}{4s\beta}[10.8 + 0.4 + 0.07] = 3\mu b. \tag{13}$$

We can see that the quark-substructure terms together with the interference terms give only the small corrections to the contribution of the Born terms, composing 4% of the total cross section.

For the neutral pions we obtain the very small cross section

$$\sigma^{\pi\pi^\circ\to\gamma\gamma} = \frac{\pi\alpha^2}{4\beta s}\cdot 0.07 = 0.02\mu b. \tag{14}$$

Now let us consider this process in dense matter. Then we can choose such values of μ, when the real part of the denominator in (4) goes to zero. Using the results of the paper [16] we can see that for $\mu = 276$ MeV, $T = 100$ MeV, $M_\pi = 160$ MeV, $m = 150$ MeV, $F_\pi = 61$ MeV

$$M_\sigma^2 - 4M_\pi^2(1+0.1) = 0 \quad , \quad m = 0.92M_\pi \ . \tag{15}$$

Here we again consider the case, $s = 0.115$ GeV^2 however now $\varepsilon = 0.1$ and $\beta = 0.3$. Then instead of Eqs (11-13) we obtain

$$\begin{aligned} s^2|\mathcal{A}|^2 &= 0.007(1 + [\frac{40m^2}{M_\sigma\Gamma_\sigma} \approx 44]^2)f_1^2 = 14.1\cdot f_1^2 \qquad (16) \\ s\mathrm{Re}\mathcal{A} &= -0.085\cdot f_2, \\ \sigma^{\pi^+\pi^-\to\gamma\gamma} &= \frac{\pi\alpha^2}{4\beta s}[14.2 - 0.16f_2 + 14.1\cdot f_1^2 \approx 21] \approx 10\mu b. \qquad (17) \end{aligned}$$

Here we put $Z\cos^2\gamma \approx 1, f_1 = 0.7$. We see that the contributions of the structure terms are comparable with the Born terms and the total cross-section increases 3.3 times. The cross section of the neutral pions increases 175 times and becomes comparable with the one of the charge pions.

$$|A|^2 s^2 = 0.007[1936 + 100 = 2036]f_1^2 = 15f_1^2 = 7.3, \tag{18}$$

$$\sigma^{\pi^0\pi^0\to\gamma\gamma} = \frac{\pi\alpha^2}{4\beta s}(15\cdot f_1^2 = 7.3) \approx 3.5\ \mu b. \tag{19}$$

The total radiation of the pion gas increases 4.5 times compared with the case where $\mu = 0$. We can observe the radiation of the photons with the energy $\omega \approx 170$ MeV.

In the Appendix I it is shown that the amplitude $\pi\pi - \gamma\gamma$ has no other singularities for all values μ and T (The Mott point singularity is absent in the box and triangle diagrams).

3. Compton effect of pions at the Mott point

The Compton effect of the charge pion is described by the Born diagrams (Fig. 1) and the diagrams describe the pion structure (Figs. 2 - 3). From these diagrams only the box diagrams 2 b-d and the vector pole and axial-vector pole diagrams 3 a-b contain the singularities at the Mott point. The box diagrams 2 b-d contain the maximal singularities at this point (see Appendix II) and in future we shall consider only these diagrams in order to describe the behaviour of the Compton effect at this point.

The Compton effect of the neutral pion is described by the structure diagrams 2 a-d and 3a, b and we also shall consider only the box diagrams in the vicinity of the Mott point.

The pole behaviour of the diagram with the σ-meson 2a disappears for the Compton effect because this part of the amplitude takes the form (see (4))

$$A^\sigma = \frac{10}{(3\pi F_\pi)^2}\frac{m^2}{(M_\sigma^2 + 2q_1q_2)}. \tag{20}$$

Now let us show that the box diagram indeed contains the strong singularity at the Mott point.

In the Appendix II we have shown that all box diagrams describing the Compton effect off pions contain terms of the type

$$C\int_o^1 d^4x\frac{\delta(\sum_i^4 x_i-1)f(x_2,x_3,x_4)}{D_1^2}, \tag{21}$$

where D_1, has the form [17] (see Fig. 4)

$$D_1 = m^2 - sx_1x_3 - tx_2x_4 - M_\pi^2x_1(x_2+x_4), \tag{22}$$

and the identical forms for the other box diagrams, there $s=(k_1+q_1)^2$, $t=(k_1-k_2)^2$, $u=(k_1-q_2)^2$ and $s+t+u=2M_\pi^2$. In the region of the small k_i where we investigate the Compton effect we can set $s\approx u\approx M_\pi^2$ and $M_\pi^2 >> -t\approx 0$.

Then D_1 takes the form

$$D_1 \approx m^2 - M_\pi^2x_1(1-x_1) \tag{23}$$

and we can integrate over x_1 in the eq. (21).

$$\frac{1}{m^4}\int_0^1\frac{dx_1}{[1-\rho x_1(1-x_1)]^2} = \frac{2}{m^4(4-\rho)}\Big[1+ \\ +\frac{4}{\sqrt{\rho(4-\rho)}}\,\mathrm{atan}\sqrt{\frac{\rho}{4-\rho}}\Big]. \tag{24}$$

Here $\rho=\frac{M_\pi^2}{m^2}$ and we see that the term contains the singularity of the type

$$\frac{const}{(4-\rho)^{3/2}} \tag{25}$$

at the Mott point where $M_\pi^2=4m^2$.

The other terms of the box diagrams and the vector (axial-vector) pole diagrams also can contain the Mott singularities however the more weak type

$$\int_0^1\frac{dx_1}{D_1} = \frac{4}{m^2\sqrt{\rho(4-\rho)}}\,\mathrm{atan}\sqrt{\frac{\rho}{4-\rho}} \tag{26}$$

and we are allowed to neglect those terms.

Contributions of the box diagrams to the amplitude of the Compton effect at the vicinity of the Mott point is of the form

$$T_\pi^{box}\mid_{\rho\approx 4} = \frac{d}{(4-\rho)^{3/2}}e_\mu(k_1)e_\nu(k_2)\Big[a_\pi(k_1^\nu.k_2^\mu - g^{\mu\nu}k_1k_2)m^2 + \\ +b_\pi(k_1q_1\cdot k_2^\mu q_1^\nu + k_1^\nu q_1^\mu\cdot q_1k_2 - k_2k_1\cdot q_1^\mu q_1^\nu - k_1q_1\cdot k_2q_1\cdot g^{\mu\nu})\Big]. \tag{27}$$

Here the new gauge invariant structure appears in eq. (27) in comparison with eq. (3) where we considered only $k^2(q^2)$ approximation. Now we consider all terms containing the lowest degrees of the k_i. The coefficient d near the Mott point is equal to

$$d\mid_{\rho\approx 4} = \frac{8\alpha}{F_\pi^2m^2}[1-\frac{1}{1+e^{\frac{m-\bar\mu}{\bar T}}}]\mid_{\bar\mu=\mu_{Mott},\bar T=T_{Mott}}. \tag{28}$$

The coefficients a_π and b_π are calculated in the Appendix II and equal

$$\begin{aligned} a_{\pi^\pm} &= \frac{26}{144}, \\ a_{\pi^0} &= \frac{125}{144}, \\ b_{\pi^\pm} &= \frac{95}{576}, \\ b_{\pi^0} &= \frac{50}{576}. \end{aligned} \tag{29}$$

Now let us calculate the cross section of the Compton scattering effect off pions at the vicinity of the Mott point and discuss the different phenomena and processes where we could observe this singular behaviour of the amplitude $\gamma\pi\to\gamma\pi$.

For the square of the amplitude (27) we obtain

$$\mid T_\pi^{box}\mid^2 = \frac{d^2}{(4-\rho)^3}(\mid d_\pi\mid^2 2(k_1k_2)^2m^4 + 2m^2M_\pi^2\,\mathrm{Re}\,(a_\pi b_\pi)(k_1k_2)^2 + \\ +\mid b_\pi\mid^2[(M_\pi^2k_1k_2 - k_1q_1\cdot k_2q_1)^2 + (k_1q_1)^2(k_2q_1)^2]). \tag{30}$$

Using the coordinate system where $k_i=(\omega_i,\omega_i\frac{\vec{k_i}}{|\vec{k_i}|})$, $k_1k_2=\omega_1\omega_2(1-c)$, $c=\cos(\vec{k_1},\vec{k_2})$, $q_1=(M_\pi,0,0,0)$, $k_iq_1=\omega_iM_\pi$ we can rewrite eq. (30) in the form

$$\mid T_\pi^{box}\mid^2 = \frac{d^2\omega_1^2\omega_2^2}{(4-\rho)^3}(2(1-c)^2\mid a_\pi\mid^2 m^4$$

$$+ \quad 2(1-c)^2 m^2 M_\pi^2 \,\mathrm{Re}\,(a_\pi b_\pi) + (1+c^2) M_\pi^4 (b_\pi)^2)$$
$$\approx \quad 2\frac{(8\omega_1\omega_2\alpha\cdot\Delta)^2}{F_\pi^4(4-\rho)^3}((1-c)^2 \mid a_\pi \mid^2 + 4(1-c)^2 \,\mathrm{Re}\,(a_\pi b_\pi) +$$
$$+ \quad 8(1+c^2) \mid b_\pi \mid^2)\Big|_{\rho\approx 4}, \qquad (31)$$

where

$$\Delta = 1 - \frac{1}{1+e^{\frac{m-\mu}{T}}} \qquad (32)$$

At $T = 100$ MeV, $\mu = 305$ MeV, $m = 95$ MeV, $M_\pi = 193$ MeV, $F_\pi = 39$ MeV, $\Delta = 0.11$; at $T = 150$ MeV, $\mu = 223$ MeV, $m = 93$ MeV, $M_\pi = 186$, $F_\pi = 40$ MeV, $\Delta = 0.3$ [16]. The last set of the date corresponds to a fit of hadron spectrum at CERN SPS experiments [19].

Calculating the cross section of this process we obtain

$$\frac{d\sigma^{Compt}}{dc} = (\frac{\omega_2}{\omega_1})^2 \frac{\mid T \mid^2}{64\pi M_\pi^2}. \qquad (33)$$

The cross section for the Born terms has the form

$$\frac{d\sigma_B^{\gamma\pi^\pm\to\gamma\pi^\pm}}{dc} = \pi\frac{\alpha^2}{M_\pi^2}(\frac{\omega_2}{\omega_1})^2(1+c^2),$$
$$\frac{\omega_2}{\omega_1} = (1+\frac{\omega_1}{M_\pi}(1-c))^{-1}, \qquad (34)$$

$$\frac{d\sigma_B^{\gamma\pi^0\to\gamma\pi^0}}{dc} = 0. \qquad (35)$$

Now let us write the cross section for the box diagrams at the vicinity of the Mott point

$$\frac{d\sigma_{box}^{\gamma\pi\to\gamma\pi}}{dc} = \frac{2}{\pi}(\frac{\alpha\omega_2^2\Delta}{M_\pi F_\pi^2})^2 \frac{1}{(4-\rho)^3}((1-c)^2[\mid a_\pi \mid^2$$
$$+ \quad 4\,\mathrm{Re}\,(a_\pi b_\pi^*)] + 8(1+c^2) \mid b_\pi \mid^2)\mid_{\rho\approx 4}. \qquad (36)$$

For the neutral mesons this cross section is four times larger then for the charged mesons and the both cross sections can contribute more than the cross section for the Born terms at the vicinity of the Mott point

$$\frac{d\sigma_{box}^{\gamma\pi^\pm\to\gamma\pi^\pm}}{d\sigma_B^{\gamma\pi^\pm\to\gamma\pi^\pm}} \sim \frac{2\cdot\Delta^2}{(4-\rho)^3},$$
$$\frac{d\sigma_{box}^{\gamma\pi^0\to\gamma\pi^0}}{d\sigma_B^{\gamma\pi^+\to\gamma\pi^+}} \sim \frac{8.6\cdot\Delta^2}{(4-\rho)^3} \qquad (37)$$

with $\omega \approx 100$ MeV, $\frac{(\omega_1\omega_2)^2}{F_\pi^4} \approx 40$ and $c = 0$.

Let us discuss the two different possibilities where we could observe this effect.

4. The change of the photon spectra of the photon-pion gas the heavy-ion collisions.

If the chemical potential of the matter after the heavy-ion collision will be $\mu \approx 233$ MeV, $T = 150$ MeV then $M_\pi = 186$ MeV, $m \approx 93$ MeV [16] and the Mott singularities appear when $M_\pi \approx 2m$. Then the photons begin to scatter very intensively off pions and their energy (frequency) decreases noticeably. In the case when the number of pions exceeds the number of photons in an equilibrium plasma then the interesting phenomenon of a shift of the photon spectrum may occur. For $\omega_1/M_\pi = 0.54, \omega_1 \approx 100$ MeV:

$$\frac{\Delta\omega}{\omega_1} = \frac{(\omega_1 - \bar{\omega}_2)}{\omega_1},$$
$$= 1 - \int_{-1}^{1} dc \frac{\omega_2}{\omega_1}\frac{d\sigma_{Box}}{dc} / \int_{-1}^{1} dc \frac{d\sigma_{Box}}{dc} \approx 0.33. \qquad (38)$$

In the case when the number of photons exceeds the number of pions this effect leads to the increasing of the dispersion in the (gaussian) photon spectra of the plasma.

5. Appearance of the possibility of observation of the "equivalent photon" scattering off the pion gas.

Consider the photons connected with the ion electrons. We can not observe them if they do not scatter off external objects. However, through the Compton effect off the pion gas these photons become observable (see Fig. 5).

Let us calculate the cross section of the process $e\pi \to e\pi\gamma(\omega_2, c)$, where ω_2 is the photon energy and $c = \cos(\vec{n}\vec{k}_2)$. $\vec{n}$ is the axis of the ion cluster and $\vec{k}_2$ is the photon momentum.

The probability of finding of the photon with the energy ω_1 in the electrons with the energy ε which fly together with ions is [18]

$$dn(x) = \frac{Z^2\alpha}{\pi}\ln(\frac{4\varepsilon^2}{m_e^2})\frac{dx}{x}(1-x+\frac{x^2}{2}), \tag{39}$$

terms has the form where Z is the number of the electrons on the ion, accompanying of one, ε is the electron energy. If we have 100 GeV per nucleon in the ion cluster then $\varepsilon = 100 \cdot m_e = 50$ MeV where m_e is the electron mass. $x = \frac{\omega_1}{\varepsilon}$, ω_1 is the energy of the photon radiated by the electron and ω_2 is the energy of the photon after scattering off the pion

$$\frac{dx}{x} = \frac{d\omega_2}{\omega_2}(1-\frac{\omega_2}{M_\pi}(1-c))^{-1}. \tag{40}$$

In the Weizsäcker–Williams [18] approximation we obtain

$$\begin{aligned} \frac{\omega_2}{\omega_1} &= [1+\frac{\omega_1}{M_\pi}(1-c)]^{-1}, \\ d\sigma^{e\pi\to e\pi\gamma} &= dn(x)\frac{d\sigma^{Compt}}{dc}, \end{aligned} \tag{41}$$

and for the cross section of the process $e\pi \to e\pi\gamma$ we get

$$\begin{aligned} \frac{d\sigma^{e\pi\to e\pi\gamma}}{dcd\omega_2} &= \frac{Z^2\alpha}{\pi}\ln(\frac{4\varepsilon^2}{m_e^2})\frac{1}{a}(1-\frac{\omega_2}{\varepsilon a}+\frac{1}{2}(\frac{\omega_2}{\varepsilon a})^2)\frac{2\omega_2}{\pi}(\frac{\alpha\omega_2}{M_\pi F_\pi^2})^2 \times \\ &\times \frac{1}{(4-\rho)^3}[(1-c)^2[|\, a_\pi\,|^2+4a_\pi b_\pi]+8(1+c^2)b_\pi^2], \end{aligned} \tag{42}$$

where $a = 1-\frac{\omega_2}{M_\pi}(1-c)$.

At the Mott point we shall observe an intensive radiation of the photons with the energy

$$\omega_2 \sim \varepsilon = 100 \cdot m_e \sim 50 MeV, \tag{43}$$

if the ion cluster has 100 GeV per nucleon and the chemical potential of the medium is ~ 305 MeV, $T = 100$ MeV, or for instance $\mu = 223$ MeV and $T = 152.5$ MeV.

6. Conclusions

We have investigated the processes $\pi\pi \to \gamma\gamma$ and $\gamma\pi \to \gamma\pi$ in a hot and dense hadronic medium. We have shown that the behaviour of these processes at large

chemical potential ($\mu > 200$ MeV) is very different. Indeed in the first case (process $\pi\pi \to \gamma\gamma$) at large μ when $M_\sigma \approx 2M_\pi$ the σ- pole diagram begin to play a very important role and other quark-substructure diagrams (box diagrams and vector (axial-vector) pole diagrams) have not any singularity behaviour in this domain. On the other hand, in the second case (process $\gamma\pi \to \gamma\pi$) the σ- pole diagram does not play any important role because the pole behaviour of this diagram disappears in this process. However, strong singularities appear in the box diagrams and in the vector (axial-vector) pole diagrams at the Mott point where $M_\pi \approx 2m$. Especially strong singularities appear in the box diagrams ($T_{box} \sim \frac{c}{(M_\pi^2-4m^2)^{3/2}}$).

The inner properties of the box diagrams, connected, for instance, with the Mott singularity can play an important role in the domain where we have a large μ. Indeed, the confinement potential is weak in this domain and can not strongly influence on the box diagram. The strong coupling constant is $g_\pi = 2.55$ in this domain (see Sect. 2), $\alpha_\pi = \frac{g_\pi^2}{4\pi} \approx 0.5$ and we can use perturbation theory. Therefore the role of the box diagram increases.

Taking into account these properties of the σ-pole and the box diagrams we give in this paper some proposals for experimental tests of them in a heavy-ion experiments.

For the process $\pi\pi \to \gamma\gamma$ we propose to measure the additional radiation of the photons with the energy $160MeV < \omega < 180$ MeV at $250 < \mu < 300$MeV.

For the process $\gamma\pi \to \gamma\pi$ we propose to measure the dispersion of the photon spectra, in the plasma where the maximum of the spectra has been shifted at $\mu = 230$ MeV by about 30 %.We also could observe the appearance of "equivalent photon" scattering off the pion gas during a heavy-ion collisions.

This is only part of the possible experiments devoted to testing of the properties of the σ-meson, pions and quarks and their behaviour in the dense matter.

We are grateful to J. Hufner for fruitful discussions. One of us (M.K.V.) acknowledges financial support provided by INTAS Grant No. W 94-2915 and the Max-Planck-Gesellschaft and the hospitality of the MPG Arbeitsgruppe "Theoretische Vielteilchenphysik" at the Rostock Universität where part of this work has been done. E.A. Kuraev acknowledges financial support provided by RFFI Grant No. 96–02–17512 and A. Arbuzov and A. Belitsky for help.

Appendix I

Let us show that in the processes $\pi\pi \to \gamma\gamma$ the box quark diagrams have not the Mott singularity at the point $M_\pi = 2m$ at finite temperature T_M or chemical potential μ_M.

Consider the box diagram described on Fig. 6

$$T_{box}^1 = ie^2g_\pi^2\frac{8}{(2\pi)^4}e_\mu^1 e_\nu^2\int d^4k\frac{N_1^{\mu\nu}}{(k^2-m^2)((k-q_2)^2-m^2)}$$

$$\times \frac{1}{((k+q_1-k_1)^2-m^2)((k+q_1)^2-m^2)}, \tag{44}$$

where

$$\begin{aligned} N_1^{\mu\nu} &= \frac{1}{4}\,\mathrm{Tr}\,\{(k+m)\gamma_5(k-q_2+m)\gamma^\nu(k+q_1-k_1+m)\times \\ &\times\ \gamma^\mu(k+q_1+m)\gamma_5\}, \end{aligned} \tag{45}$$

q_1, q_2 are the momenta of the incoming pions and k_1, k_2 are the momenta of the outgoing photons. k is the internal momentum of the quark.

After the transformations

$$\begin{aligned} \frac{1}{a_1a_2a_3a_4} &= 6\int_0^1 d\tau_4 (\sum_{i=1}^4 a_i x_i)^{-4}, \\ d\tau_4 &= d^4x\,\delta(\sum_{i=1}^4 x_i - 1) \end{aligned} \tag{46}$$

and the replacement $k = k' + b$, where

$$b = x_4k_2 + (x_3+x_4)k_1 - (x_2+x_3+x_4)q_1, \tag{47}$$

we can integrate over d^4k in (44) using the formulae

$$\begin{aligned} \int \frac{d^4k}{(k^2-D_1)^4} &= i\frac{\pi^2}{6D_1^2}; \\ \int d^4k \frac{k^\nu k^\mu}{(k^2-D_1)^4} &= -i\pi^2\frac{g^{\mu\nu}}{12D_1}, \end{aligned} \tag{48}$$

where

$$\begin{aligned} &D_1 = m^2 - sx_2x_4 - tx_1x_3 - M_\pi^2 x_1(x_2+x_4), \\ &s = (k_1+k_2)^2, \quad t = (k_1-q_1)^2; u = (k_1-q_2)^2, \\ &s+t+u = 2M_\pi^2. \end{aligned} \tag{49}$$

Let us consider the part of the amplitude (44) which contains the combination of the photon momenta $k_1^\nu k_2^\mu$. It takes the form

$$\Delta T_{box}^{(1)} = -e^2g^2\frac{\pi^2}{(2\pi)^4}e_1^\mu e_2^\nu \int d\tau_4 \left[\frac{m^2k_1^\nu k_2^\mu B_1 + A_1^{\mu\nu}}{D_1^2} - k_1^\nu k_2^\mu \frac{C_1}{2D_1}\right], \tag{50}$$

where

$$\begin{aligned} B_1 &= 2x_4(x_3+x_4) - 3x_4 - x_3 + 1, \\ C_1 &= -16x_4(x_3+x_4) + 18x_4 + 6x_3 - 4, \\ A_1^{\mu\nu} &= -\frac{1}{4}\,\mathrm{Tr}\,(b(b-q_2)\gamma^\nu(b+q_1-k_1)\gamma^\mu(b+q_1). \end{aligned} \tag{51}$$

In $A_1^{\mu\nu}$ we conserve only terms contain $k_1^\nu k_2^\mu$. The total amplitude has to contain the gauge inv. expression $(k_1^\nu k_2^\mu - g^{\mu\nu}k_1k_2)$.

Now we investigate the form

$$I_1 = \int_0^1 \frac{d\tau_4}{D_1^2} \tag{52}$$

which could contain the maximal singularities at the Mott point where $M_\pi^2 = 4m^2$. Consider this form near the threshold where $s \approx 4M_\pi^2$, $t \approx 0, (\rho = \frac{M_\pi^2}{m^2})$:

$$\begin{aligned} I_1 &= \int \frac{dx_1dx_2dx_4\theta(1-x_1-x_2-x_4)}{[1-\rho(4x_2x_4+x_1(x_2+x_4))]^2} = \\ &= \rho^{-3/2}\int_0^1 \frac{du}{u}\Big[\frac{1}{\sqrt{1-\rho u}}\,\mathrm{atan}\,[u\sqrt{\frac{\rho}{1-\rho u}}] \\ &- \frac{1}{\sqrt{1-\rho u^2}}\,\mathrm{atan}\,[u\sqrt{\frac{\rho}{1-\rho u^2}}]\Big]. \end{aligned} \tag{53}$$

This integral does not contain a singularity at the value $\rho = 4$ (the Mott point). Other parts of the amplitude describing the process $\pi\pi \to \gamma\gamma$ also have not the singularities at this point.

Appendix II

Consider the Compton effect off the pion using the quark box diagrams (Figs. 4,7)

After the transformation (46) and the exchange

$$k = k' + b \tag{54}$$

we obtain (after integration over d^4k').

$$T_{box} = -\frac{2e^2g^2Q_q^2}{(2\pi)^2}\int d\tau_4 [\frac{N_1^{\mu\nu}}{D_1^2} + \frac{N_2^{\mu\nu}}{D_2^2} + \frac{N_3^{\mu\nu}}{D_3^2}]e_\mu^1 e_\nu^2, \tag{55}$$

where Q_q is the charge operator of the quark

$$\begin{aligned} D_1 &= m^2 - sx_1x_3 - tx_2x_4 - M_\pi^2x_1(x_2+x_4), \\ D_2 &= m^2 - tx_1x_3 - sx_2x_4 - M_\pi^2x_2(x_3+x_1), \\ D_3 &= m^2 - sx_1x_3 - ux_2x_4 - M_\pi^2(x_1x_2+x_3x_4), \end{aligned} \tag{56}$$

$$N_1^{\mu\nu} = \frac{i}{4}\,\mathrm{Tr}\,(\gamma^5(b_1+m)\gamma^5(b_1+q_2+m)\times$$
$$\times\ \gamma^\nu(b_1+q_1+k_1+m)\gamma^\mu(b_1+q_1+m)),$$

$$N_2^{\mu\nu} = \frac{1}{4}\,\mathrm{Tr}\,(\gamma^5(b_3+m)\gamma^\mu(b_3-k_1+m)\times$$
$$\times\ \gamma^\nu(b_3+q_1-q_2+m)\gamma^5(b_3+q_1+m)),$$

$$N_3^{\mu\nu} = \frac{1}{4}\,\mathrm{Tr}\,(\gamma^5(b_2+m)\gamma^\nu(b_2+k_2+m)\times$$
$$\times\ \gamma^5(b_2+q_1+k_1+m)\gamma^\mu(b_2+q_1+m),$$

$$b_1 = -x_2q_1 - x_3(q_1+k_1) - x_4q_2,$$
$$b_3 = -x_2q_1 - x_3(q_1+k_1) - x_4k_2,$$
$$b_2 = -x_2q_1 - x_3(q_1-q_2) - x_4k_1.$$

The eq. (55) contains only the maximal singular parts of the amplitude $\pi\gamma \to \pi\gamma$ at the Mott point:

$$s = (k_1+q_1)^2, \quad t=(k_1-k_2)^2, \quad u=(k_1-q_2)^2, \qquad (57)$$
$$s \approx u \approx M_\pi^2, \quad t \approx 0.$$

In the domain of the small k_i the all D_i take the form (23) and after the integration over x_1 (or $u = x_1 + x_4$ for D_3) the amplitude (55) takes the form (24), where we have singularities of the type (25) at the Mott point.

The numerators of the eq. (55) contain the two types of the gauge invariant structures in the k^2 approximation

$$T_1^{\mu\nu} = -k_1^\nu k_2^\mu + g^{\mu\nu}k_1k_2,$$

$$T_2^{\mu\nu} = k_1q_1k^\mu q_1^\nu + k_2q_1\cdot k_1^\nu q_1^\mu - k_1k_2q_1^\nu q_1^\mu - k_1q_1\cdot k_2q_1\cdot g^{\mu\nu}. \qquad (58)$$

The other parts of the (55) disappears through gauge invariance. The coefficients before these structures in N_i have the forms

$$N_i^{\mu\nu} = N_i^{(1)}T_1^{\mu\nu} + N_i^{(2)}T_2^{\mu\nu}; \qquad (59)$$

$$N_1^{(1)} = N_2^{(1)} = m^2(1-2x_4)(1-x_3-x_4)$$
$$+\ M_\pi^2[(1-x_1)^2(2x_4-1)(1-x_3-x_4) + (x_3+x_4)(x_1+x_4)$$
$$+\ (1-x_3-x_4)(1-x_1-x_4) - x_4],$$

$$N_3^{(1)} = m^2(1-x_3-x_4) + M_\pi^2[(x_2+x_3)^2(x_3+x_4-1)$$
$$-\ 2x_3(1-x_1) + 2x_3 + x_2]. \qquad (60)$$

At the Mott point we can put $x_1 = \frac{1}{2}$ in the eq. (59) and $x_2 + x_3 = \frac{1}{2}$ in the eq. (60). Then after integration over x_i we obtain

$$\int d\tilde{x} = \int_0^{\frac{1}{2}} dx_3 \int_0^{\frac{1}{2}-x_3} dx_4,$$

$$\int dx N_1^{(1)} = \int dx N_2^{(1)} = m^2[\frac{11}{4\cdot 48} + \rho\frac{17}{16\cdot 48}]\,|_{\rho=4} = m^2\frac{7}{48},$$

$$\int dx N_3^{(1)} = m^2[\frac{4}{48} + \rho\frac{7}{4\cdot 48}]\,|_{\rho=4} = \frac{11}{48} \qquad (61)$$

The coefficients before the second structure have the forms

$$N_1^{(2)} = N_2^{(2)} = 2x_1[2(1+x_1)(x_3+x_4)x_4 - x_3 - 2x_4],$$

$$N_3^{(2)} = 2[x_2x_4 + x_1x_3]$$

and

$$\int dx N_1^{(2)} = \int dx N_2^{(2)} = -\frac{5}{2\cdot 64},$$

$$\int dx N_3^{(2)} = \frac{5}{3\cdot 64} \qquad (62)$$

Taking into account the quark charges we obtain for the coefficients a_π and b_π the values given in (29):

$$a_{\pi_0} = \frac{1}{2}\frac{5}{3}\left\{4\left(\frac{7}{48}\right) + 2\left(\frac{11}{48}\right)\right\} = \frac{125}{144};$$
$$a_{\pi_\pm} = 2\left(\frac{4}{3}+\frac{1}{3}\right)\left(\frac{7}{48}\right) + 2\left(-\frac{2}{3}\right)\left(\frac{11}{48}\right) = \frac{13}{72};$$
$$b_{\pi_0} = \frac{1}{2}\frac{5}{3}\left\{4\left(\frac{5}{128}\right) - 2\left(\frac{5}{192}\right)\right\} = \frac{25}{288};$$
$$b_{\pi_\pm} = 2\left(\frac{4}{3}+\frac{1}{3}\right)\left(\frac{5}{128}\right) + 2\left(\frac{2}{3}\right)\left(\frac{5}{192}\right) = \frac{95}{576}. \qquad (63)$$

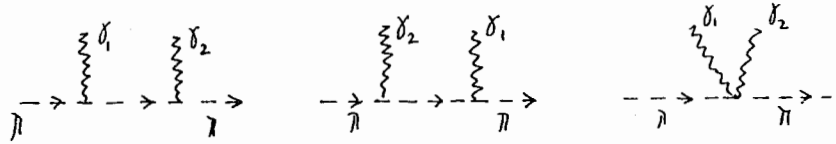

Fig. 1 Born Feynman diagrams for the pion Compton scattering.

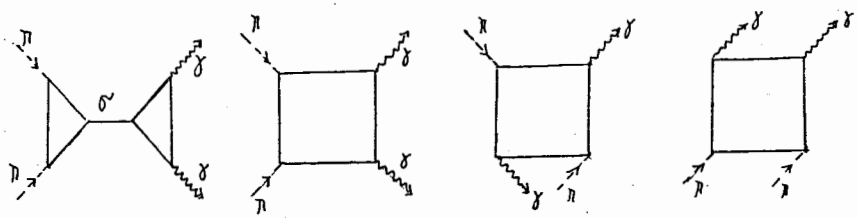

Fig. 2 Two–photon annihilation of pions.

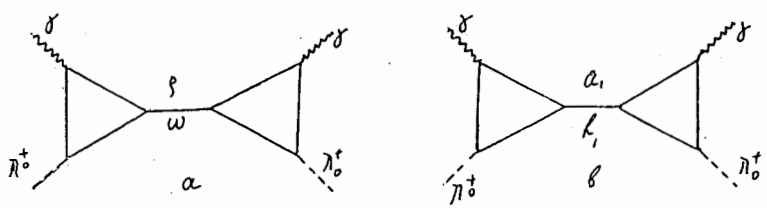

Fig. 3 Vector–meson contribution to pion Compton scattering diagrams.

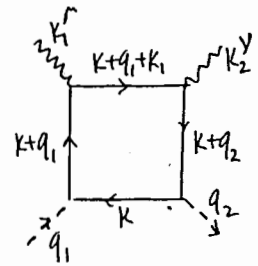

Fig. 4 Typical box diagrams for pion Compton scattering.

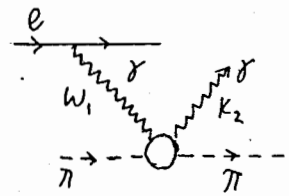

Fig. 5 Inelastic electron-pion scattering.

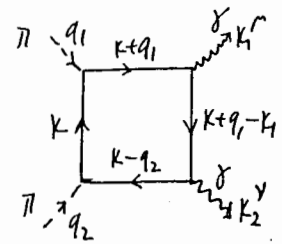

Fig. 6 Box diagram for two-quantum annihilation of pions.

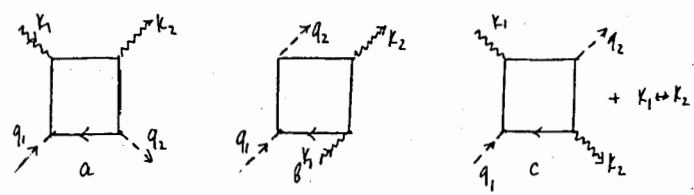

Fig. 7 Feynman diagrams for the pion Compton scattering.

References

[1] T. Matsui and H. Satz, Phys.Lett. **B 178** (1986) 416.

[2] CERES Collab., G. Agakichiev et al., Phys. Rev. Lett. **75** (1995) 1272.

[3] J. Rafelski and B. Müller, Phys. Rev. Lett. **48** (1982) 1066.

[4] C. Gale and J. Kapusta Phys. Rev. C 35, (1989), 2107.

[5] G.Q. Li, C.M.Ko and G.E. Brown, Phys. Rev. Lett. **75** (1995) 4007.

[6] H.-J. Schulze and D. Blaschke, *Dilepton Enhancement by Thermal Pion Annihilation in the CERES Experiment*, nucl.-th/9607055.

[7] R. Baier, M. Dirks and K. Redlich, *Thermal Dileptons from $\pi - -\rho$ Interactions in a Hot Pion Gas*, hep-ph/9610210.

[8] Review of Part Properties, Phys. Rev. D 50 (1994) 1198; Phys.Rev. D54 (1996) 1.

[9] M. Svec, A. de Lesqnen, L. van Rossum, Phys. Rev. D46 (1992) 949;
M. Svec, HEP-Preprint, hep-ph/9511205, Nov. 1995.

[10] S. Ishida et al., Prog. Theor. Phys. 95 (1996) 745.

[11] M.K. Volkov, Sov. J. Part. and Nucl. 17 (1986) 186.

[12] M.K. Volkov and A.A. Osipov, Sov. J. Nucl. Phys. 41 (1985) 659.

[13] Y. Nambu, G. Jona-Lasinio, Phys. Rev. 122 (1961) 345;
D. Ebert, M.K. Volkov, Sov. J. Nucl. Phys. 36 (1982) 736; Z. Phys. C16 (1983) 205;
M.K. Volkov, Ann. Phys. (NY) 159 (1984) 282;
D. Ebert, H. Reinhard, Nucl. Phys. B271 (1986) 188;
D. Ebert, A.N. Ivanov, M.K. Volkov, Fortschr. Phys. 37 (1989) 487;
H. Vogl, W. Weise, Progr. Part. Nucl. Phys. 27 (1991) 195;
S.P. Klevansky, Rev. Mod. Phys. 64 (1992) 649;
T. Hatsuda and T. Kunihiro, Phys. Rep. **247** (1994) 221;
D. Ebert, H. Reinhard, M.K. Volkov, Progr. Part. Nucl. Phys. A 576 (1994) 1;

[14] A.E. Dorokhov,J. Huffner,S.P. Klevansky,M.K. Volkov Preprint Heidelberg Univ., HD-TVP-95-12, Heidelberg, 1995;Chinese J.Phys.34 (1996) 901;
A.E. Dorokhov et al. to be published in Z.Phys.C.

[15] D. Ebert and M.K. Volkov, JINR preprint E 2-96-119, Dubna, 1996; hep-ph/9604396; Yad.Fiz. 60 (1997) N 4;
D. Ebert,T. Feldman,M.K. Volkov, DESY 96-074, April, 1996 (to be published in Int.J.Mod.Phys.A).

[16] D. Ebert, Yu.L. Kalinovsky, L. Münchow and M.K. Volkov, Int. J. Mod. Phys. A 8 (1993) 1295.

[17] R.J. Eden, P.V. Landshoff, D.I. Olive and J.C. Polkinghorne, The Analytic S-Matrix, Cambridge, England, 1966.

[18] A.I. Akhiezer, V.B. Berestetsky — "Quantum electrodynamics", GIFML, Moscow, 1959.

[19] J. Sollfrank,Dissertation,Regensburg,1994,unpublished.For recent parametrizations of freeze-out temperatures and chemical potentials see P. Brown-Munzinger,J. Stachel,J.P. Wessels and N. Xu, Physl. Lett. **B 305** (1996) 1.

Received by Publishing Department on December 18, 1996.